

Enhanced petrogenic organic carbon oxidation during the Paleocene-Eocene thermal maximum

E.H. Hollingsworth, R.B. Sparkes, J.M. Self-Trail, G.L. Foster, G.N. Inglis

Supplementary Information

The Supplementary Information includes:

- Table S-1 and S-2
- Figure S-1 and S-2
- Supplementary Information References

Table S-1 Number of disordered carbon vs. graphitised carbon spectra from SDB, with duplicate results in parenthesis. The disordered and graphitised carbon were separated based on peak burial temperatures, which were calibrated using the R2 and RA2 peak area ratio (see Sparkes *et al.*, 2013). The time intervals are as follows: Pre-PETM, PETM (onset/body), Recovery, and Post-PETM, based on Hollingsworth *et al.* (2024) and references therein. The pre-onset Excursion (POE) in the Pre-PETM interval is isolated using the definition from Babila *et al.* (2022).

Time interval	Approx. sample depth (m)	Disordered carbon	Graphitised carbon
Post-PETM	186.6	5	5
Post-PETM	188	7	3
Recovery	190.99	6	3
Recovery	192.57	5	5
Recovery	193.3	5	5
Recovery	193.88	2	7
Recovery	195.07	5	5
Recovery	196.41	3	7
PETM	196.93	3	7
PETM	197.21	2 (4)	8 (6)
PETM	199.52	3	7
PETM	199.83	4	6
PETM	200.28	2	8
PETM	200.83	2	7
PETM	201.47	3	6
PETM	202.08	3	7
PETM	202.37	4 (9)	6 (1)
PETM	202.68	7	3
PETM	202.98	5	4
PETM	203.06	7 (7)	3 (2)
PETM	203.3	6	3
PETM	203.88	9	1
Pre-PETM	204.26	9	1
Pre-PETM	204.49	8	2
Pre-PETM	204.84	8	2
Pre-PETM	205.12	9 (9)	1 (1)
Pre-PETM	205.4	8	2
Pre-PETM	205.44	8	2
Pre-PETM	205.74	7	3
POE	206.04	8	2
POE	206.35	9	1
POE	206.41	5	4
POE	206.68	9	1
POE	207.04	5	5
POE	207.08	7	3
Pre-PETM	208.83	7	3

Table S-2 Number of disordered carbon vs. graphitised carbon spectra from ACEX. The disordered and graphitised carbon were separated based on peak burial temperatures, which were calibrated using the R2 and RA2 peak area ratio (see Sparkes *et al.*, 2013). The time intervals are as follows: Pre-PETM, PETM (onset/body), Recovery, and Post-PETM, based on Hollingsworth *et al.* (2024) and references therein.

Time interval	Depth (mcd)	Freeze-dried	Oven-dried	Disordered carbon	Graphitised carbon
Post-PETM	378.14	Yes		9	1
Recovery	378.69		Yes	10	0
Recovery	380.73	Yes		10	0
Recovery	381.56	Yes		9	1
PETM	382.15		Yes	9	1
PETM	382.94		Yes	8	1
PETM	383.87		Yes	10	0
PETM	385.11		Yes	10	0
Pre-PETM	388.03		Yes	10	0
Pre-PETM	388.87	Yes		10	0
Pre-PETM	389.75		Yes	10	0
Pre-PETM	390.78	Yes		10	0

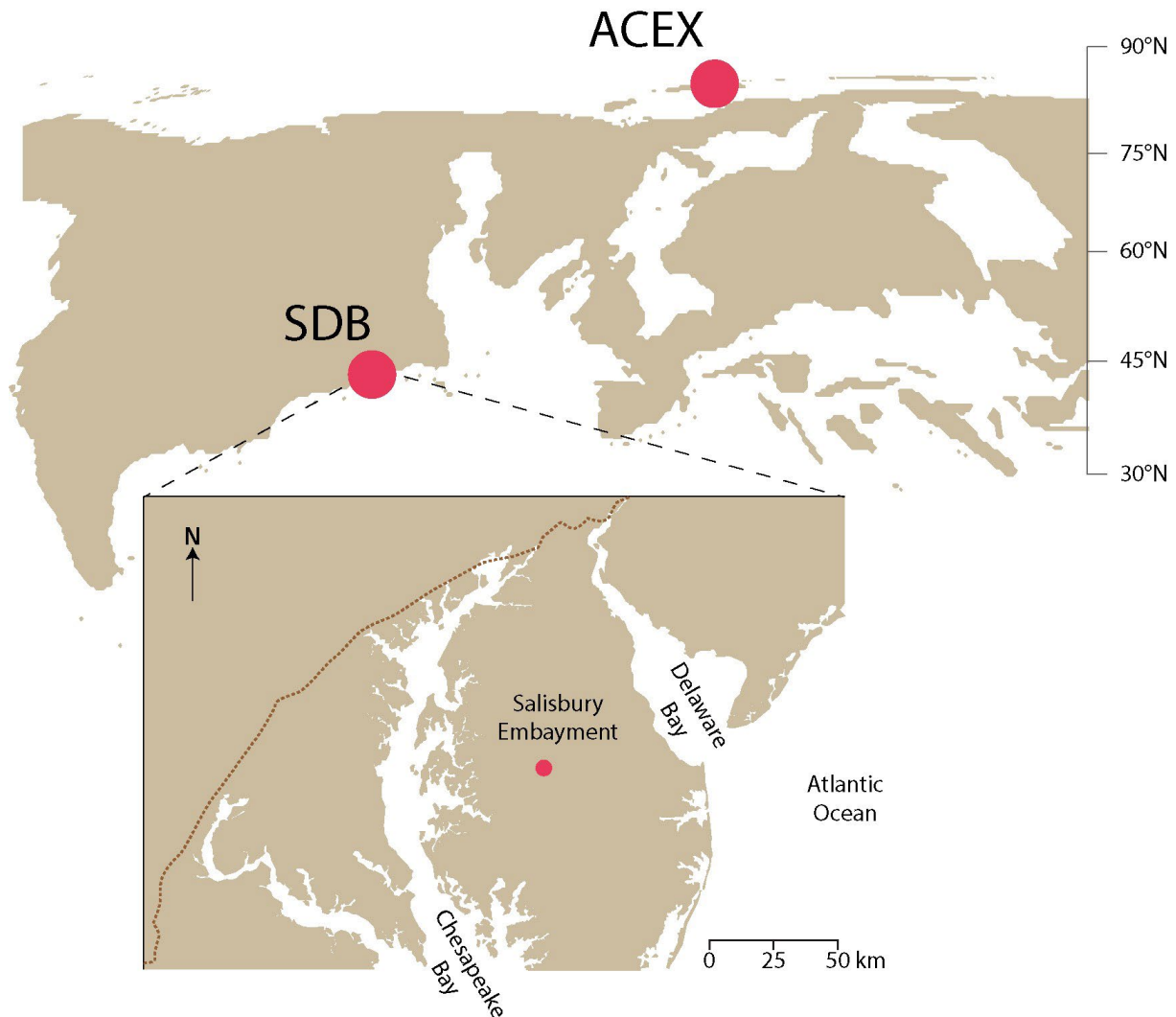


Figure S-1 Location of the Arctic Coring Expedition (ACEX; 82.81°N, 66.91°E) and South Dover Bridge (SDB; 41.39°N, 59.48°W) during the PETM (palaeo-latitudes based on mantle reference frame; Hollis *et al.*, 2019). Top panel: representation of the palaeogeography of the Northern Hemisphere 56 Ma, adapted from Carmichael *et al.* (2017). Bottom panel: the mid-Atlantic Coastal Plain with the modern coastline and Fall Line (brown dashed line).

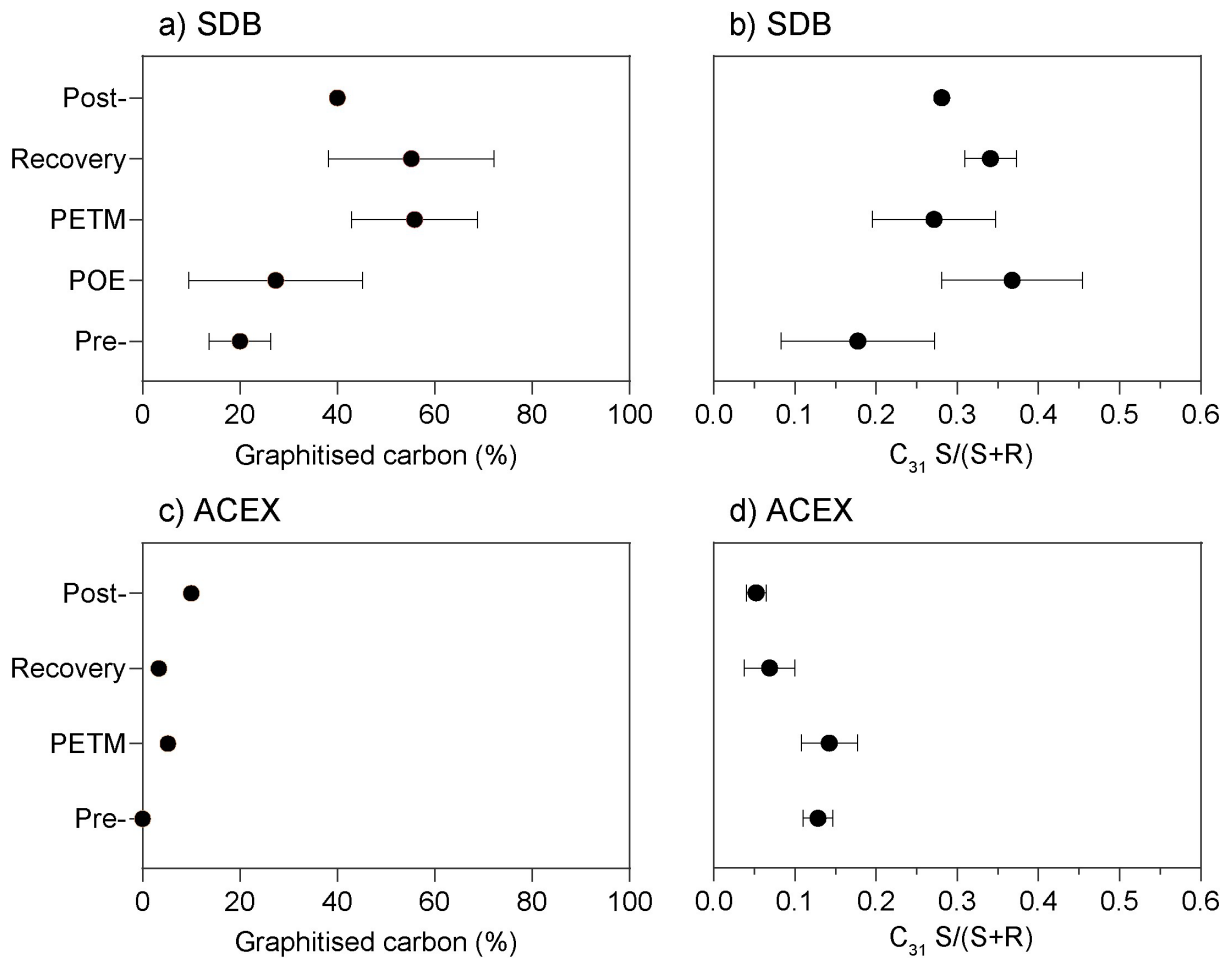


Figure S-2 Mean percentages of graphitised carbon (this study) and mean values of the C_{31} homohopane $22S/(22S+22R)$ ratio (Lyons *et al.*, 2019; Hollingsworth *et al.*, 2024), from (a-b) SDB and (c-d) ACEX. The time intervals are as follows: Pre-PETM, PETM (onset and body), Recovery, and Post-PETM (see Hollingsworth *et al.*, 2024 and references therein). At SDB, the POE in the Pre-PETM interval is isolated using the definition from Babila *et al.* (2022). The uncertainty is displayed as the 95 % confidence interval of the mean, with error bars not included when sample size is < 4 .

Supplementary Information References

- Babila, T.L., Penman, D.E., Standish, C.D., Doubrawa, M., Bralower, T.J., *et al.* (2022) Surface ocean warming and acidification driven by rapid carbon release precedes Paleocene-Eocene Thermal Maximum. *Science Advances* 8. <https://doi.org/10.1126/sciadv.abg1025>
- Carmichael, M.J., Inglis, G.N., Badger, M.P.S., Naafs, B.D.A., Behrooz, L., Rimmelzwaal, S., Monteiro, F.M., Rohrsen, M., Farnsworth, A., Buss, H.L., Dickson, A.J., Valdes, P.J., Lunt, D.J., Pancost, R.D. (2017) Hydrological and associated biogeochemical consequences of rapid global warming during the Paleocene-Eocene Thermal Maximum. *Global and Planetary Change* 157, 114–138. <https://doi.org/10.1016/j.gloplacha.2017.07.014>
- Hollingsworth, E.H., Elling, F.J., Badger, M.P.S., Pancost, R.D., Dickson, A.J., *et al.* (2024) Spatial and Temporal Patterns in Petrogenic Organic Carbon Mobilization During the Paleocene-Eocene Thermal Maximum. *Paleoceanography and Paleoclimatology* 39. <https://doi.org/10.1029/2023PA004773>
- Hollis, C.J., Dunkley Jones, T., Anagnostou, E., Bijl, P.K., Cramwinckel, M.J., *et al.* (2019) The DeepMIP contribution to PMIP4: Methodologies for selection, compilation and analysis of latest Paleocene and early Eocene climate proxy data, incorporating version 0.1 of the DeepMIP database. *Geoscientific Model Development* 12, 3149–3206. <https://doi.org/10.5194/gmd-12-3149-2019>
- Lyons, S.L., Baczynski, A.A., Babila, T.L., Bralower, T.J., Hajek, E.A., *et al.* (2019) Palaeocene–Eocene Thermal Maximum prolonged by fossil carbon oxidation. *Nature Geoscience* 12, 54–60. <https://doi.org/10.1038/s41561-018-0277-3>
- Sparkes, R.B., Hovius, N., Galy, A., Kumar, R.V., Liud, J.T. (2013) Automated analysis of carbon in powdered geological and environmental samples by Raman spectroscopy. *Applied Spectroscopy* 67, 779–788. <https://doi.org/10.1366/12-06826>